
This is the **accepted version** of the article:

Ren, Ping; Rossi, Sergio; Camarero, J. Julio; [et al.]. «Critical temperature and precipitation thresholds for the onset of xylogenesis of *Juniperus przewalskii* in a semi-arid area of the northeastern Tibetan Plateau». *Annals of Botany*, Vol. 121, Issue 4 (March 2018), p. 617-624. DOI 10.1093/aob/mcx188

This version is available at <https://ddd.uab.cat/record/218314>

under the terms of the  **CC BY** COPYRIGHT license

Title: Critical temperature and precipitation thresholds for the onset of xylogenesis of *Juniperus przewalskii* in a semi-arid area of the northeastern Tibetan Plateau

Running head: Thresholds for the onset of xylogenesis

PING REN^{1,2}, SERGIO ROSSI^{3,4}, J. JULIO CAMARERO⁵, AARON M. ELLISON⁶,
ERYUAN LIANG^{1,2,7}, JOSEP PEÑUELAS^{8,9}

¹*Key Laboratory of Alpine Ecology and Biodiversity, Institute of Tibetan Plateau Research, Chinese Academy of Sciences, Beijing 100101, China*

²*Key Laboratory of Tibetan Environment Changes and Land Surface Processes, Institute of Tibetan Plateau Research, Chinese Academy of Sciences, Beijing, 100101, China;*

³*University of Quebec in Chicoutimi, Département des Sciences Fondamentales, 555, Boulevard de l'Université, Chicoutimi (QC) G7H2B1, Canada*

⁴*Key Laboratory of Vegetation Restoration and Management of Degraded Ecosystems, Guangdong Provincial Key Laboratory of Applied Botany, South China Botanical Garden, Chinese Academy of Sciences, Guangzhou 510650, China*

⁵*Instituto Pirenaico de Ecología (IPE, CSIC), Avda. Montañana 1005, 50080 Zaragoza, Spain*

⁶*Harvard University, Harvard Forest, 324 North Main Street, Petersham, MA 01366, USA*

⁷*CAS centre for Excellence in Tibetan Plateau Earth Sciences, Beijing 100101, China*

⁸*CSIC, Global Ecology Unit CREAF-CSIC-UAB, Bellaterra, E-08193 Catalonia, Spain;*

⁹*CREAF, Cerdanyola del Vallès, E-08193 Catalonia, Spain*

Correspondence: Eryuan Liang, tel. +86 10 84097069, fax +86 10 84097079, e-mail:

liangey@itpcas.ac.cn

29 Abstract

30 The onset of xylogenesis plays an important role in tree growth and carbon
31 sequestration at the level of ecosystems and is thus a key to modeling the responses of
32 forest ecosystems to climate change. Temperature regulates the resumption of cambial
33 activity, but little is known about the effect of water availability on the onset of
34 xylogenesis. We monitored the onset of xylogenesis during 2009–2014 by weekly
35 microcoring *Juniperus przewalskii* trees at the upper and lower altitudinal limits of the
36 species on the northeastern Tibetan Plateau. A logistic regression was used to
37 calculate the probability of xylogenic activity at a given temperature. A
38 two-dimensional reversed Gaussian model was used to fit the differences between the
39 observed date of onset of xylogenesis and days at given temperatures and
40 precipitation within a certain time window. The thermal thresholds at the beginning of
41 the growing season were highly variable, providing additional evidence that
42 temperature was not the only factor initiating xylem growth under cold and dry
43 climatic conditions. The onset of xylogenesis was predicted well for climatic
44 thresholds characterized by a cumulative precipitation of 17.0 ± 5.6 mm and an
45 average minimum temperature of 1.5 ± 1.4 °C for a period of 12 days. Xylogenesis in
46 semi-arid regions with dry winters and springs can start when both critical
47 temperature and precipitation thresholds are reached. Such findings contribute to our
48 knowledge of the environmental drivers of growth resumption that were previously
49 investigated only in regions with abundant snow accumulation in winter and frequent
50 precipitation in spring. Models of the onset of xylogenesis should include water

51 availability for more reliable predictions of xylem phenology in dry areas. A
52 mismatch of the thresholds of temperature and moisture for the onset of xylogenesis
53 may increase forest vulnerability in semi-arid areas under droughts due to global
54 climate change.

55

56 *Keywords: Phenology, xylem formation, Qilian juniper, two-dimensional Gaussian*
57 *model, drought, rain, altitudinal gradient*

58

59 **Introduction**

60 Interest in xylem phenology (xylogenesis) and its sensitivity to climate change is
61 growing because wood is a major sink of carbon in terrestrial ecosystems (Babst *et al.*,
62 2014; Cuny *et al.*, 2015; Pérez-de-Lis *et al.*, 2017). Temperature is increasingly
63 recognized as the primary driver of growth reactivation in cold climates (Rossi *et al.*,
64 2007, 2008). Both observations and controlled experiments have demonstrated that
65 cambial activity is limited by low air temperatures in cold climates (Oribe *et al.*, 2001;
66 Gricar *et al.*, 2006; Rossi *et al.*, 2008; Seo *et al.*, 2008; Gruber *et al.*, 2010; Begum *et*
67 *al.*, 2013; Li *et al.*, 2013). In addition, the onset of xylem production is delayed at
68 higher latitudes and altitudes, confirming the role of temperature for xylogenesis
69 (Moser *et al.*, 2010; Oladi *et al.*, 2010; Huang *et al.*, 2011). In particular, Rossi *et al.*
70 (2008) reported a critical daily minimum temperature for xylogenesis in conifers of
71 4–5 °C in cold climates. Shen *et al.* (2015), though, highlighted the impact of
72 precipitation on the starting date of vegetation phenology (canopy greening) in cold
73 and arid or semi-arid regions, indicating that cold and drought stress both affected the
74 onset of growth. Ren *et al.* (2015) found a delay in the initiation of xylogenesis in
75 Qilian junipers (*Juniperus przewalskii* Kom.) under extremely dry spring conditions
76 in a cold and dry climate, which suggested a potential influence of water availability
77 on the start of xylogenesis, i.e. on the onset of cambial reactivation after the cold
78 dormant season (winter in the Northern Hemisphere).

79 The effect of precipitation on the growth dynamics of forest ecosystems needs to
80 be quantified to better understand the adaptation of plants to a changing climate,

81 which may be characterized by warmer and drier conditions (Allen *et al.*, 2015). In
82 addition, the climatic thresholds for the resumption of xylem phenology may provide
83 keys to better understand mechanisms of forest resilience (e.g. post-drought recovery)
84 and the potential for tipping points under global change. Water acts on several
85 important growth processes in plants. The expansion of xylem cells is turgor-driven,
86 depending on the uptake of cellular water and on solute accumulation. Drought stress
87 affects the loss of turgor of differentiating cells (Kozlowski & Pallardy, 2002), so
88 shifts in the onset of xylogenesis might be potentially affected by variation in
89 moisture conditions, especially in the arid and semi-arid regions of the world. The
90 available literature, however, is limited to studies conducted in regions characterized
91 by rains prior to the onset of xylogenesis (from winter to spring), such as the
92 Mediterranean basin (Camarero *et al.*, 2010, 2015; Vieira *et al.*, 2013), or by abundant
93 water released during snowmelt, such as alpine valleys (Gruber *et al.*, 2010; Eilmann
94 *et al.*, 2011; Swidrak *et al.*, 2011). Soil moisture could be a less important limiting
95 factor for the resumption of xylem formation at these sites than in arid or semi-arid
96 areas. We investigated how cold and dry conditions could drive the onset of
97 xylogenesis by determining the relative influence of these two climatic stressors.

98 We selected a forested area on the northeastern Tibetan Plateau to test the effect of
99 soil moisture on the onset of xylogenesis. The dry climate of this area is characterized
100 by scarce winter precipitation, a very thin snowpack and the dependence of moisture
101 availability for vegetation activity on the first rains of spring (Dai, 1990). The climate
102 is described as cold and dry, with a mean annual temperature of 3.1 °C and a mean

103 annual precipitation of ca. 200 mm. Winter is extremely dry, and rain mainly falls
104 from May to September (Dai, 1990). The Qilian juniper forests in this area are
105 stressed by both drought and cold (Zheng *et al.*, 2008). A recent study reported that
106 spring drought could delay the onset of xylogenesis in Qilian juniper despite optimal
107 thermal conditions (Ren *et al.*, 2015). In addition, warmer spring conditions on the
108 plateau are increasing the vulnerability of forests to dry spells, indicated by a marked
109 decrease in growth and an increase in the frequency of missing tree rings (Liang *et al.*,
110 2014, 2016). These findings suggested a potential interaction between precipitation
111 and temperature in the onset of xylogenesis under cold and dry conditions.

112 The objective of this study was to use Qilian juniper as a model species to
113 investigate the onset of xylogenesis at the upper and lower altitudinal boundaries of
114 its distribution during six growing seasons (2009-2014) and to identify the thresholds
115 of temperature and precipitation controlling the onset of xylogenesis. We
116 hypothesized that the onset of xylogenesis in Qilian juniper was constrained more by
117 water deficit than by low temperatures.

118

119 **Materials and Methods**

120 *Study site, field sampling and sample preparation*

121 The study was carried out in an undisturbed Qilian juniper forest near Dulan County
122 on the northeastern Tibetan Plateau (36°00'N, 98°11'E). Two sites, at 3850 and 4210
123 m a.s.l. with slopes of 15°, were selected at the lower and upper timberline limits of
124 the altitudinal distribution of the species. Five trees were randomly selected at each

125 site. The average diameter at breast height was 50–60 cm, and the average height was
126 8 m. Microcores were extracted weekly from 2009 to 2014 from the stems at a height
127 of 1.0-1.3 m using a Trephor microborer (Rossi *et al.*, 2006) and stored in a
128 formalin–ethanol–acetic acid solution. The microcores were prepared to obtain
129 transverse sections (9-12 μm in thickness) using a Leica RM 2245 rotary microtome
130 (Leica Microsystems, Wetzlar, Germany), and the sections were stained using a
131 mixture of safranin, Astra Blue and ethanol and then permanently fixed. See Ren *et*
132 *al.* (2015) for more details on sampling strategy and slide preparation.

133

134 *Identification of the onset of xylogenesis*

135 The xylem sections were observed under a microscope at a magnification of 100 \times
136 with visible and polarized light to distinguish the differentiating xylem cells. We
137 concentrated on the radial-enlargement phase, which indicates the beginning of xylem
138 growth (Antonova & Stasova, 1993). Tracheids in the radial-enlarging phase
139 contained a protoplast enclosed in thin primary cell walls, and their radial diameters
140 were at least twice that of a cambial cell (Rossi *et al.*, 2006). The tracheids had
141 light-blue walls under normal light during this phase but were not visible under
142 polarized light due to the lack of a secondary wall. Xylogenesis was considered to
143 have begun for each tree when at least one radial file of enlarging cells was observed
144 in spring.

145

146 *Meteorological data*

147 Meteorological data were recorded at each site from October 2012 by automatic
148 stations (HOBO; ONSET, Pocasset, USA). Air temperature and precipitation were
149 measured every 30 min and stored in data loggers. Minimum, mean, and maximum
150 daily temperatures and daily precipitation were calculated for subsequent analyses.
151 Data for January 2009 to September 2012 were estimated using the measurements
152 collected from a meteorological station in Dulan (36°18'N, 98°06'E; 3190 m a.s.l.), 32
153 km from the study sites. The consistency of the estimates was based on the high
154 correlations ($r > 0.92$) between the climatic data (temperature and precipitation) at the
155 two sites with those at the Dulan station (Supporting Information, Fig. S1).

156

157 *Statistical analyses to predict climatic thresholds of xylogenesis*

158 Based on previous research (Ren *et al.*, 2015), air temperature and precipitation were
159 selected as potential climatic drivers of the beginning of xylogenesis.

160 Logistic regression was used to calculate the probability of xylogenic activity at a
161 given temperature using the LOGISTIC procedure in the SAS 9.4 statistical package
162 [SAS Institute Inc., Cary, USA]. See Rossi *et al.* (2007, 2008) for more details on the
163 calculation of temperature thresholds and model verification. The model was fitted
164 with the minimum, mean, and maximum temperatures for each tree, site and year.
165 None of 180 models applied was excluded because of a lack of fit (in all cases
166 $R^2 > 0.90$). Thermal thresholds were then compared between years using an ANOVA.

167 Two-dimensional reversed Gaussian models were used to calculate the difference
168 between the onset of xylogenesis and the day with a given temperature and

169 precipitation within a certain time window. The Gaussian model generates a
 170 funnel-surface plot, with a circular-to-elliptical cross-section with the general form:

$$171 \quad Z_{xy} = Z_0 - A \exp\left(-\frac{1}{2} \left(\frac{xcos\theta + ysin\theta - x_c cos\theta - y_c sin\theta}{W_1} \right)^2 - \frac{1}{2} \left(\frac{-xsin\theta + ycos\theta + x_c sin\theta - y_c cos\theta}{W_2} \right)^2 \right)$$

172 where Z_{xy} is the mean absolute difference between the day of onset of xylogenesis and
 173 the estimated day with a given average temperature x and cumulative precipitation y
 174 within the time window t across trees, sites and years, Z_0 is the distance from the edge
 175 of the surface to the plane $z = 0$, A is the height of the trough, x_0 and y_0 are the
 176 coordinates defining the position of the center of the surface, W_1 and W_2 are the
 177 spreads of the surface on the x - and y -axes, respectively, and θ is the clockwise
 178 rotation angle of the surface (see Supporting Information, Fig. S2). The model was
 179 fitted with the corresponding temperature (minimum, mean and maximum air
 180 temperatures) and precipitation series for each time window. The culmination of the
 181 coefficient of determination (R^2) of the model was considered to correspond to the
 182 optimal time window t . The critical average temperature (x) and cumulative
 183 precipitation (y) were calculated when Z_{xy} was near 0 at the optimal time window t .
 184 Standardized residuals were calculated for model verification. Model validation was
 185 performed by comparing the observations (onset of xylogenesis) with the predicted
 186 values calculated using data for precipitation and temperature as predictors.

187

188 **Results**

189 *Spring meteorological conditions*

190 The daily mean temperatures in March at the upper and lower sites were -4.7 and

191 -3.2 °C, respectively, reaching 1.8 and 3.4 °C in May. Monthly precipitation, on
192 average, increased tenfold, from 5–6 mm in March to 50–60 mm in May (Supporting
193 Information, Fig. S3).

194 Spring (March to May) conditions varied between years (Fig. S3). The warmest
195 spring during the study was in 2009, with daily mean temperatures reaching 1.4 and
196 -0.2 °C at the lower and upper sites, respectively. The coldest and driest springs were
197 in 2014, with mean temperatures of -0.2 and -1.8 °C and total precipitation of 25.8
198 and 31.0 mm at the lower and upper sites, respectively. Monthly precipitation in
199 March 2014 ranged between 17.4 and 21.8 mm, which represented the highest amount
200 of spring rain during the study period.

201

202 *Threshold temperatures*

203 The threshold temperature with a probability of 0.5 for active xylogenesis was
204 calculated as an average for each year and site (Table 1). Thermal thresholds at the
205 lower site varied within large ranges, 0-5, 4-9 and 10-14 °C for the daily minimum,
206 mean and maximum temperatures, respectively. Thresholds were significantly higher
207 in 2010 than in other years and were lowest in 2014 ($P<0.001$). The thermal
208 thresholds were lower at the upper site, but also with large ranges, 0–5, 3–8 and
209 8–12 °C for the daily minimum, mean and maximum temperatures, respectively. The
210 thresholds at the upper site also differed significantly between years ($P<0.001$).
211 Thresholds were significantly higher in 2010 than the other years and were lower in
212 2014 for the daily minimum and mean temperatures and in 2012 and 2014 for the

213 maximum temperature.

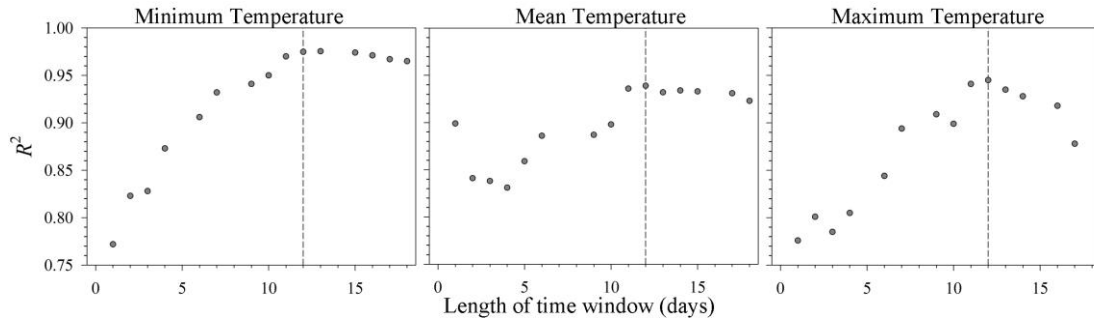
214 **Table 1** Threshold minimum, mean and maximum temperatures corresponding to
 215 95% probability of active xylogenesis in *Juniperus przewalskii* estimated during
 216 2009-2014 at the lower and upper study sites. Results from an ANOVA are reported as
 217 *F* and *P*. Different letters within a row indicate significant differences at $P < 0.05$.

Site	Temperat ure (°C)	2009	2010	2011	2012	2013	2014	F	P
		Lower	Minimum	2.5 ± 0.4 ^a	5.0 ± 0.7 ^b	2.4 ± 0.7 ^a	1.8 ± 0.4 ^a		
	Mean	7.2 ± 0.4 ^a	9.3 ± 0.8 ^b	7.5 ± 0.7 ^a	6.0 ± 0.4 ^a	6.3 ± 0.9 ^a	4.5 ± 0.7 ^c	26.33	<0.001
	Maximum	12.0 ± 0.5 ^a	14.2 ± 0.9 ^b	12.0 ± 1.0 ^a	10.0 ± 0.4 ^c	11.3 ± 0.9 ^{a,c}	9.8 ± 0.8 ^c	21.80	<0.001
Upper	Minimum	1.9 ± 0.2 ^{a,b}	4.5 ± 0.3 ^c	2.4 ± 0.4 ^a	1.0 ± 0.6 ^b	1.2 ± 0.9 ^b	-0.5 ± 0.4 ^d	53.83	<0.001
	Mean	5.9 ± 0.2 ^{a,b}	8.0 ± 0.3 ^c	6.4 ± 0.3 ^a	4.5 ± 0.6 ^d	5.0 ± 0.9 ^{b,d}	3.4 ± 0.4 ^e	52.06	<0.001
	Maximum	10.1 ± 0.2 ^{a,b}	12.2 ± 0.3 ^c	10.8 ± 0.5 ^a	7.9 ± 0.6 ^d	9.4 ± 0.9 ^b	8.1 ± 0.4 ^d	51.31	<0.001

218

219 *Two-dimensional Gaussian models*

220 R^2 of the Gaussian models varied with the length of the time window (Fig. 1). R^2
 221 increased for longer time windows, culminating with a time window of 12 days when
 222 R^2 reached 0.97, 0.99 and 0.94 for the minimum, mean and maximum temperatures,
 223 respectively. R^2 decreased slightly (minimum and mean temperature) or substantially
 224 (maximum temperature) for time windows longer than 12 days.



225

226 **Fig. 1** Coefficient of determination (R^2) for the two-dimensional Gaussian models

227 within the time window from 1 to 18 days. Dotted lines indicate the time windows (in

228 days) corresponding to maximum R^2 .

229

230 The minimal Z_{xy} was 2.21 days for a time window of 12 days. The critical

231 cumulative precipitation was 17.0 ± 5.6 mm and the average minimum temperature

232 was 1.5 ± 1.4 °C when Z_{xy} was <2.5 days (Fig. 2). The spreads of this trough on the x -

233 and y -axes were 48.0 mm and 2.04 °C, respectively, with a counter-clockwise rotation

234 of 4.73°. In the model with the average mean temperature, the minimal Z_{xy} was 1.85

235 days. The critical precipitation and temperature were 26.9 ± 3.9 mm and 4.6 ± 1.8 °C,

236 respectively when Z_{xy} was <2 days. The spreads of this trough on the x - and y -axes

237 were 44.1 mm and 1.94 °C respectively, with a counter-clockwise rotation of 8.22°.

238 The minimal Z_{xy} was 1.90 days in the model with the average maximum temperature.

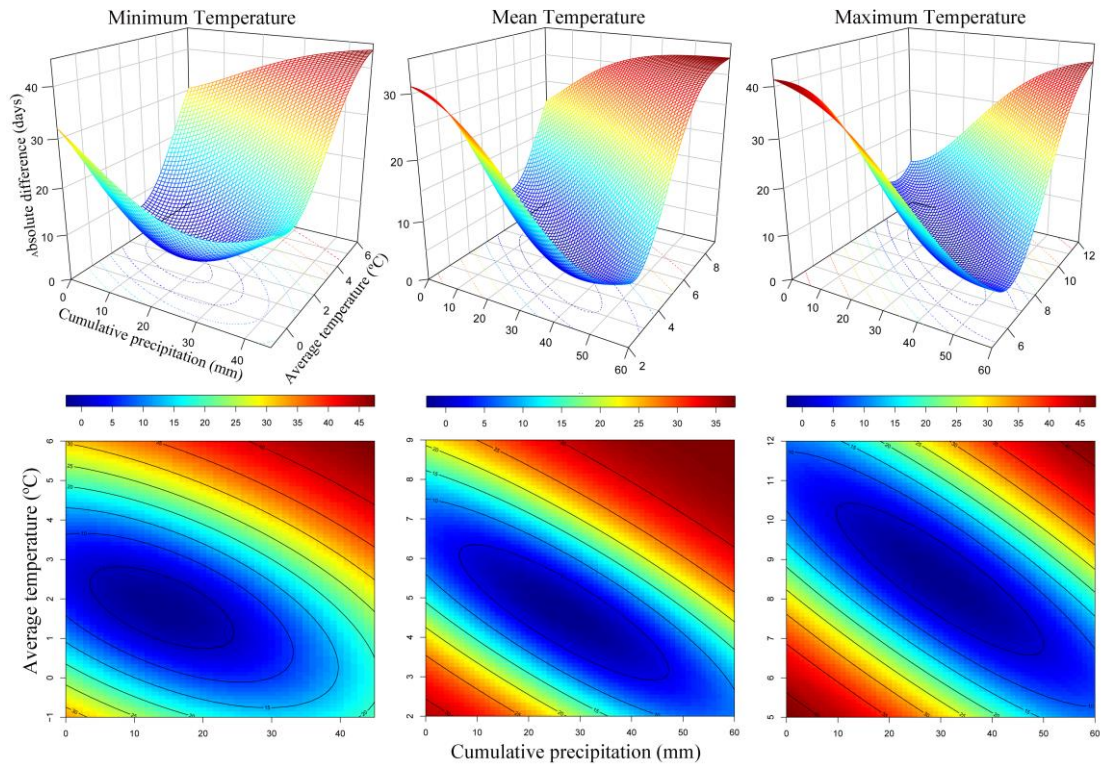
239 The critical precipitation and temperature were 29.9 ± 3.0 mm and 8.5 ± 1.8 °C,

240 respectively, when Z_{xy} was <2 days. The spreads of this trough on the x - and y -axes

241 were 51.1 mm and 2.39 °C, respectively, with a counter-clockwise rotation of 9.52°.

242 Most of the standardized residuals of these three models converged from -2 to 2

243 (Supporting Information, Fig. S4).

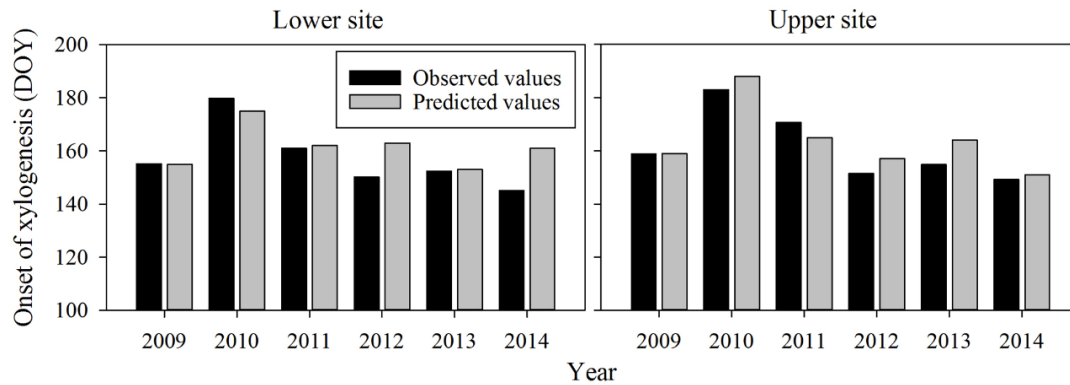


244

245 **Fig. 2** Surface plots and the corresponding level sets showing the two-dimensional
 246 Gaussian distribution of the absolute difference between the day of onset of
 247 xylogenesis and the estimated day with a given average temperature and cumulative
 248 precipitation in the time window of 12 days. Note that the axes have different scales.

249

250 The absolute differences between the observed and predicted dates of onset of
 251 xylogenesis using average minimum temperature and cumulative precipitation in a
 252 time window of 12 days were smaller than the sampling interval by averages of 5.9
 253 and 4.6 days at the lower and upper sites, respectively (Fig. 3). The predictions for
 254 2009, 2011 and 2013 were the most reliable. The divergences between observations
 255 and predictions (16 days) were largest in 2014 at the lower site.



256

257 **Fig. 3** Observed and predicted days of onset of xylogenesis (DOY, day of the year) in

258 *Juniperus przewalskii* during 2009-2014 at the lower and upper study sites.

259 Predictions were obtained using the threshold average minimum temperature and

260 cumulative precipitation calculated by the models.

261

262 Discussion

263 We challenged the general opinion that temperature was the only driver of growth

264 reactivation at high elevations by analyzing the onset of xylogenesis of Qilian juniper

265 subjected to cold and dry climatic conditions on the northeastern Tibetan Plateau.

266 Published threshold temperatures for the onset of xylogenesis in trees range from 2 to

267 3 °C (Rossi *et al.*, 2007, 2008; Swidrak *et al.*, 2011; Boulouf Lugo *et al.*, 2012). The

268 range in the thermal thresholds of 5 °C for the onset of xylogenesis in Qilian juniper

269 provides additional evidence that temperature was not the only factor initiating xylem

270 growth under cold and dry climatic conditions. More reliable predictions were

271 attained when both thermal and precipitation thresholds for the onset of xylogenesis

272 were included in the fitted models. The interaction between temperature and

273 precipitation satisfactorily explained the day of onset of xylogenesis in 2010, which

274 was delayed by ca. three weeks compared with 2009 and 2011, despite the warm
275 conditions during that spring (Ren *et al.*, 2015). This finding suggests that spring
276 precipitation is also an important factor in the resumption of xylem formation in
277 Qilian juniper.

278 Water availability is an important determinant of xylem formation. Before the start
279 of xylem phenology, trees must compensate for the water lost during winter and
280 spring to recover an adequate water balance, because turgor is an important requisite
281 for xylem cell growth (Sevanto *et al.*, 2006). Rehydration in spring can exceed six
282 weeks, and stems are fully rehydrated one month before the onset of radial growth
283 (Turcotte *et al.*, 2009). Both cell division and expansion in the xylem are sensitive to
284 changes in water potential (Abe & Nakai, 1999; Savidge, 2001). The water potential
285 in the cambium regulates mitosis and influences cell extension and the deposition of
286 wall polymers (Abe & Nakai, 1999; Cosgrove, 2005; Arend & Fromm, 2007). Springs
287 were rainy or water was abundantly supplied by snowmelt in the cold regions of
288 previous studies, so the initiation of xylem growth was not limited by rehydration, and
289 trees responded essentially to temperature rather than precipitation (Turcotte *et al.*,
290 2009). Warmer springs in such areas can substantially advance xylem phenology
291 (Rossi *et al.*, 2011). Winter and spring are similarly often wet in cold and
292 drought-prone regions such as continental Mediterranean forests, and moisture is not
293 considered the only factor in the resumption of xylem formation (Camarero *et al.*,
294 2010). Winter is extremely dry in our study area, with scarce snow, and water
295 availability is consequently low before growth reactivation. Moreover, drought stress

296 would be higher under drier and warmer conditions, which would thus slow the onset
297 of xylogenesis, as observed in spring 2010. Soil moisture occasionally can be
298 increased by snowfall, such as the snowfall in 2014, as also occurs in boreal forests
299 (Vaganov *et al.*, 1999). The amount of water available during the snowmelt in our
300 study increased soil moisture and possibly advanced the onset of xylogenesis, likely
301 explaining the difference of 16 days between observations and predictions in 2014 at
302 the lower site. This research found that the onset of xylogenesis in Qilian juniper
303 should meet the prerequisite for both critical temperature and precipitation.

304 This study is the first to demonstrate that the onset of xylogenesis is driven by an
305 interaction between thermal and precipitation thresholds. The selected time window
306 of 12 days agrees with the period required for tracheid expansion and differentiation
307 (Vaganov *et al.*, 2006; Cuny *et al.*, 2015). Temperature is a well-recognized factor
308 controlling the onset of xylem formation, but our findings provide new insights on the
309 climatic forcing of growth. The critical temperatures and precipitation provide keys
310 for modelling the response of forest ecosystems subjected to cold and dry constraints
311 in response to climate change and would help our understanding of the regime shifts
312 in these ecosystems (Scheffer *et al.*, 2001; Zhu *et al.*, 2014). Our findings also support
313 the constraint of growth by drought stress in high-elevation forests or near the alpine
314 treeline, as indicated by previous studies (Liang *et al.*, 2014; Piper *et al.*, 2016).

315 Trees in semi-arid areas are generally limited by drought and high temperature at
316 the beginning of the growing season, which increase rates of evapotranspiration
317 (Allen *et al.*, 2015), and a similar constraint has been reported for the Tibetan Plateau

318 and other Asian mountains (Shao *et al.*, 2005; Liang *et al.*, 2006, 2016; Liu *et al.*,
319 2006; Gou *et al.*, 2014; Pederson *et al.*, 2014; Yang *et al.*, 2014; Zhang *et al.*, 2015).
320 Warming-induced drought stress has been decreasing generalized tree growth and
321 increasing mortality in semi-arid areas across Asia (Dulamsuren *et al.*, 2010; Liu *et*
322 *al.*, 2013; Liang *et al.*, 2016; Allen *et al.*, 2015). In particular, the failure to produce
323 stem wood in a particular year (missing rings) is a response to dry and warm spring
324 conditions, and an increasing frequency of missing tree rings is also evident in
325 response to the warming in recent decades (Liang *et al.*, 2014, 2016). Moreover, the
326 frequency of missing rings has been strongly linked to tree mortality (Liang *et al.*,
327 2016). We hypothesize that a failure to reach critical water availability for growth
328 reactivation or a delay in cambial resumption in response to increasing drought stress
329 could be primary factors in the failure to form a complete ring and portend lower
330 growth and forest dieback. A mismatch between critical temperatures and amounts of
331 moisture for the onset of xylogenesis under the drought conditions of global climate
332 change and the acceleration of dryland expansion (Peñuelas *et al.*, 2007; Allen *et al.*,
333 2015; Huang *et al.*, 2015) will reduce forest resilience and risk regime shifts in
334 vulnerable semi-arid forests. Reyer *et al.* (2015) proposed the assessment of forest
335 resilience and potential tipping points at various levels, from leaf to biosphere, and
336 our study has stressed that climatic thresholds for the onset of xylogenesis can be key
337 indicators of forest resilience and tipping points under changing climates.

338

339 **Acknowledgments**

340 This work was supported by the National Natural Science Foundation of China
341 (41525001, 41471158 and 41171161), and the International Partnership Program of
342 Chinese Academy of Sciences (131C11KYSB20160061). JP's research was supported
343 by the European Research Council Synergy grant ERC-2013-SyG
344 610028-IMBALANCE-P. We thank Macairangjia and Chengye He for the weekly
345 microcore sampling.

346

347 **References**

- 348 Abe H, Nakai T (1999) Effect of the water status within a tree on tracheid
349 morphogenesis in *Cryptomeria japonica* D. Don. *Trees*, **14**, 124-129.
- 350 Allen CD, Breshears DD, McDowell NG (2015) On underestimation of global
351 vulnerability to tree mortality and forest die-off from hotter drought in the
352 Anthropocene. *Ecosphere*, **6**, art129.
- 353 Antonova G, Stasova V (1993) Effects of environmental factors on wood formation in
354 Scots pine stems. *Trees*, **7**, 214-219.
- 355 Arend M, Fromm J (2007) Seasonal change in the drought response of wood cell
356 development in poplar. *Tree Physiology*, **27**, 985-992.
- 357 Babst F, Bouriaud O, Papale D *et al.* (2014) Above-ground woody carbon
358 sequestration measured from tree rings is coherent with net ecosystem
359 productivity at five eddy-covariance sites. *New Phytologist*, **201**, 1289-1303.
- 360 Begum S, Nakaba S, Yamagishi Y, Oribe Y, Funada R (2013) Regulation of cambial
361 activity in relation to environmental conditions: understanding the role of

362 temperature in wood formation of trees. *Physiologia Plantarum*, **147**, 46-54.

363 Boulouf Lugo J, Deslauriers A, Rossi S (2012) Duration of xylogenesis in black
364 spruce lengthened between 1950 and 2010. *Annals of Botany*, **110**, 1099-1108.

365 Camarero JJ, Gazol A, Sangüesa-Barreda G, Oliva J, Vicente-Serrano SM (2015) To
366 die or not to die: early warnings of tree dieback in response to a severe
367 drought. *Journal of Ecology*, **103**, 44-57.

368 Camarero JJ, Olano JM, Parras A (2010) Plastic bimodal xylogenesis in conifers from
369 continental Mediterranean climates. *New Phytologist*, **185**, 471-480.

370 Cosgrove DJ (2005) Growth of the plant cell wall. *Nature Reviews Molecular Cell
371 Biology*, **6**, 850-861.

372 Cuny HE, Rathgeber CB, Frank D *et al.* (2015) Woody biomass production lags
373 stem-girth increase by over one month in coniferous forests. *Nature Plants*, **1**,
374 1-6.

375 Dai J (1990) *The Climate of the Tibetan Plateau (in Chinese)*, Beijing, China
376 Meteorological Press.

377 Dulamsuren C, Hauck M, Leuschner C (2010) Recent drought stress leads to growth
378 reductions in *Larix sibirica* in the western Khentey. *Global Change Biology*,
379 **16**, 3024-3035.

380 Eilmann B, Zweifel R, Buchmann N, Graf Pannatier E, Rigling A (2011) Drought
381 alters timing, quantity, and quality of wood formation in Scots pine. *Journal of
382 Experimental Botany*, **62**, 2763-2771.

383 Gou X, Deng Y, Gao L, Chen F, Cook E, Yang M, Zhang F (2014) Millennium

384 tree-ring reconstruction of drought variability in the eastern Qilian Mountains,
385 northwest China. *Climate Dynamics*, **45**, 1761-1770.

386 Gricar J, Zupancic M, Cufar K, Koch G, Schmitt U, Oven P (2006) Effect of local
387 heating and cooling on cambial activity and cell differentiation in the stem of
388 Norway spruce (*Picea abies*). *Annals of Botany*, **97**, 943-951.

389 Gruber A, Strobl S, Veit B, Oberhuber W (2010) Impact of drought on the temporal
390 dynamics of wood formation in *Pinus sylvestris*. *Tree Physiology*, **30**,
391 490-501.

392 Huang J, Yu H, Guan X, Wang G, Guo R (2015) Accelerated dryland expansion
393 under climate change. *Nature Climate Change*, **6**, 166-171.

394 Huang JG, Bergeron Y, Zhai L, Denneler B (2011) Variation in intra-annual radial
395 growth (xylem formation) of *Picea mariana* (Pinaceae) along a latitudinal
396 gradient in western Quebec, Canada. *American Journal of Botany*, **98**,
397 792-800.

398 Kozłowski TT, Pallardy SG (2002) Acclimation and adaptive responses of woody
399 plants to environmental stresses. *The Botanical Review*, **68**, 270-334.

400 Li X, Liang E, Gricar J, Prislan P, Rossi S, Cufar K (2013) Age dependence of
401 xylogenesis and its climatic sensitivity in Smith fir on the south-eastern
402 Tibetan Plateau. *Tree Physiology*, **33**, 48-56.

403 Liang E, Dawadi B, Pederson N, Eckstein D (2014) Is the growth of birch at the upper
404 timberline in the Himalayas limited by moisture or by temperature? *Ecology*,
405 **95**, 2453-2465.

406 Liang E, Leuschner C, Dulamsuren C, Wagner B, Hauck M (2016) Global
407 warming-related tree growth decline and mortality on the north-eastern
408 Tibetan plateau. *Climatic Change*, **134**, 163-176.

409 Liang E, Liu X, Yuan Y *et al.* (2006) The 1920s drought recorded by tree rings and
410 historical documents in the semi-arid and arid areas of Northern China.
411 *Climatic Change*, **79**, 403-432.

412 Liu H, Park Williams A, Allen CD *et al.* (2013) Rapid warming accelerates tree
413 growth decline in semi-arid forests of Inner Asia. *Global Change Biology*, **19**,
414 2500-2510.

415 Liu Y, An Z, Ma H *et al.* (2006) Precipitation variation in the northeastern Tibetan
416 Plateau recorded by the tree rings since 850 AD and its relevance to the
417 Northern Hemisphere temperature. *Science in China Series D*, **49**, 408-420.

418 Moser L, Fonti P, Buntgen U, Esper J, Luterbacher J, Franzen J, Frank D (2010)
419 Timing and duration of European larch growing season along altitudinal
420 gradients in the Swiss Alps. *Tree Physiology*, **30**, 225-233.

421 Oladi R, Pourtahmasi K, Eckstein D, Bräuning A (2010) Seasonal dynamics of wood
422 formation in Oriental beech (*Fagus orientalis* Lipsky) along an altitudinal
423 gradient in the Hyrcanian forest, Iran. *Trees*, **25**, 425-433.

424 Oribe Y, Funada R, Shibagaki M, Kubo T (2001) Cambial reactivation in locally
425 heated stems of the evergreen conifer *Abies sachalinensis* (Schmidt) masters.
426 *Planta*, **212**, 684-691.

427 Peñuelas J, Ogaya R, Boada M, S. Jump A (2007) Migration, invasion and decline:

428 changes in recruitment and forest structure in a warming-linked shift of
429 European beech forest in Catalonia (NE Spain). *Ecography*, **30**, 829-837.

430 Pederson N, Hessel AE, Baatarbileg N, Anchukaitis KJ, Di Cosmo N (2014) Pluvials,
431 droughts, the Mongol Empire, and modern Mongolia. *Proceedings of the*
432 *National Academy of Sciences*, **111**, 4375-4379.

433 Pérez-de-Lis G, Olano JM, Rozas V, Rossi S, Vázquez-Ruiz RA, García-González I
434 (2017) Environmental conditions and vascular cambium regulate carbon
435 allocation to xylem growth in deciduous oaks. *Functional Ecology*, **31**,
436 592–603.

437 Piper FI, Viñeola B, Linares JC, Camarero JJ, Cavieres LA, Fajardo A, Wardle D
438 (2016) Mediterranean and temperate treelines are controlled by different
439 environmental drivers. *Journal of Ecology*, **104**, 691-702.

440 Ren P, Rossi S, Gricar J, Liang E, Cufar K (2015) Is precipitation a trigger for the
441 onset of xylogenesis in *Juniperus przewalskii* on the north-eastern Tibetan
442 Plateau? *Annals of Botany*, **115**, 629-639.

443 Reyer CPO, Brouwers N, Rammig A *et al.* (2015) Forest resilience and tipping points
444 at different spatio-temporal scales: approaches and challenges. *Journal of*
445 *Ecology*, **103**, 5-15.

446 Rossi S, Deslauriers A, Anfodillo T (2006) Assessment of cambial activity and
447 xylogenesis by microsampling tree species: An example at the alpine
448 timberline. *IAWA Journal*, **27**, 383-394.

449 Rossi S, Deslauriers A, Anfodillo T, Carraro V (2007) Evidence of threshold

450 temperatures for xylogenesis in conifers at high altitudes. *Oecologia*, **152**,
451 1-12.

452 Rossi S, Deslauriers A, Gričar J *et al.* (2008) Critical temperatures for xylogenesis in
453 conifers of cold climates. *Global Ecology and Biogeography*, **17**, 696-707.

454 Rossi S, Morin H, Deslauriers A, Plourde P-Y (2011) Predicting xylem phenology in
455 black spruce under climate warming. *Global Change Biology*, **17**, 614-625.

456 Savidge R (2001) Intrinsic regulation of cambial growth. *Journal of Plant Growth*
457 *Regulation*, **20**, 52-77.

458 Scheffer M, Carpenter S, Foley JA, Folke C, Walker B (2001) Catastrophic shifts in
459 ecosystems. *Nature*, **413**, 591-596.

460 Seo JW, Eckstein D, Jalkanen R, Rickebusch S, Schmitt U (2008) Estimating the
461 onset of cambial activity in Scots pine in northern Finland by means of the
462 heat-sum approach. *Tree Physiology*, **28**, 105-112.

463 Sevanto S, Suni T, Pumpanen J *et al.* (2006) Wintertime photosynthesis and water
464 uptake in a boreal forest. *Tree Physiology*, **26**, 749-757.

465 Shao X, Huang L, Liu H, Liang E, Fang X, Wang L (2005) Reconstruction of
466 precipitation variation from tree rings in recent 1000 years in Delingha,
467 Qinghai. *Science in China Series D*, **48**, 939-949.

468 Shen M, Piao S, Cong N, Zhang G, Jassens IA (2015) Precipitation impacts on
469 vegetation spring phenology on the Tibetan Plateau. *Global Change Biology*,
470 **21**, 3647-3656.

471 Swidrak I, Gruber A, Kofler W, Oberhuber W (2011) Effects of environmental

472 conditions on onset of xylem growth in *Pinus sylvestris* under drought. *Tree*
473 *Physiology*, **31**, 483-493.

474 Turcotte A, Morin H, Krause C, Deslauriers A, Thibeault-Martel M (2009) The
475 timing of spring rehydration and its relation with the onset of wood formation
476 in black spruce. *Agricultural and Forest Meteorology*, **149**, 1403-1409.

477 Vaganov EA, Hughes MK, Kirilyanov AV, Schweingruber FH, Silkin PP (1999)
478 Influence of snowfall and melt timing on tree growth in subarctic Eurasia.
479 *Nature*, **400**, 149-151.

480 Vaganov EA, Hughes MK, Shashkin AV (2006) *Growth dynamics of conifer tree*
481 *rings: images of past and future environments*, Springer-Verlag., Berlin,
482 Heidelberg, Germany.

483 Vieira J, Rossi S, Campelo F, Freitas H, Nabais C (2013) Xylogenesis of *Pinus*
484 *pinaster* under a Mediterranean climate. *Annals of Forest Science*, **71**, 71-80.

485 Yang B, Qin C, Wang J, He M, Melvin TM, Osborn TJ, Briffa KR (2014) A
486 3,500-year tree-ring record of annual precipitation on the northeastern Tibetan
487 Plateau. *Proceedings of the National Academy of Sciences*, **111**, 2903-2908.

488 Zhang QB, Evans MN, Lyu L (2015) Moisture dipole over the Tibetan Plateau during
489 the past five and a half centuries. *Nature Communications*, **6**, 8062.

490 Zheng Y, Liang E, Zhu H, Shao X (2008) Response of radial growth of Qilian juniper
491 to climatic change under different habitats. *Journal of Beijing Forestry*
492 *University*, **30**, 7-12.

493 Zhu K, Woodall CW, Ghosh S, Gelfand AE, Clark JS (2014) Dual impacts of climate

494 change: forest migration and turnover through life history. *Global Change*

495 *Biology*, **20**, 251-264.

496

497

498

499

500

501

502

503

504

505

506

507

508

509

510

511

512

513

514

515

516

517 **Supporting Information captions**

518 Fig. S1 Correlations between the daily minimum, mean and maximum temperatures
519 recorded at the Dulan meteorological station and the corresponding temperatures
520 recorded during 2012-2014 at the lower and upper study sites. ***, correlation
521 coefficients (r) at $P < 0.001$.

522

523 Fig. S2 Sample surface plot and the corresponding level sets of a two-dimensional
524 Gaussian model. In the upper plot, Z_0 is the distance from the edge of the surface to
525 the plane ($z = 0$), and A is the height of the trough. In the lower plot, x_0 and y_0 are the
526 coordinates defining the position of the center of the surface, and θ is the clockwise
527 rotation angle of the surface.

528

529 Fig. S3 Daily air temperature (lines) and precipitation (bars) during 2009-2014 at the
530 lower and upper study sites.

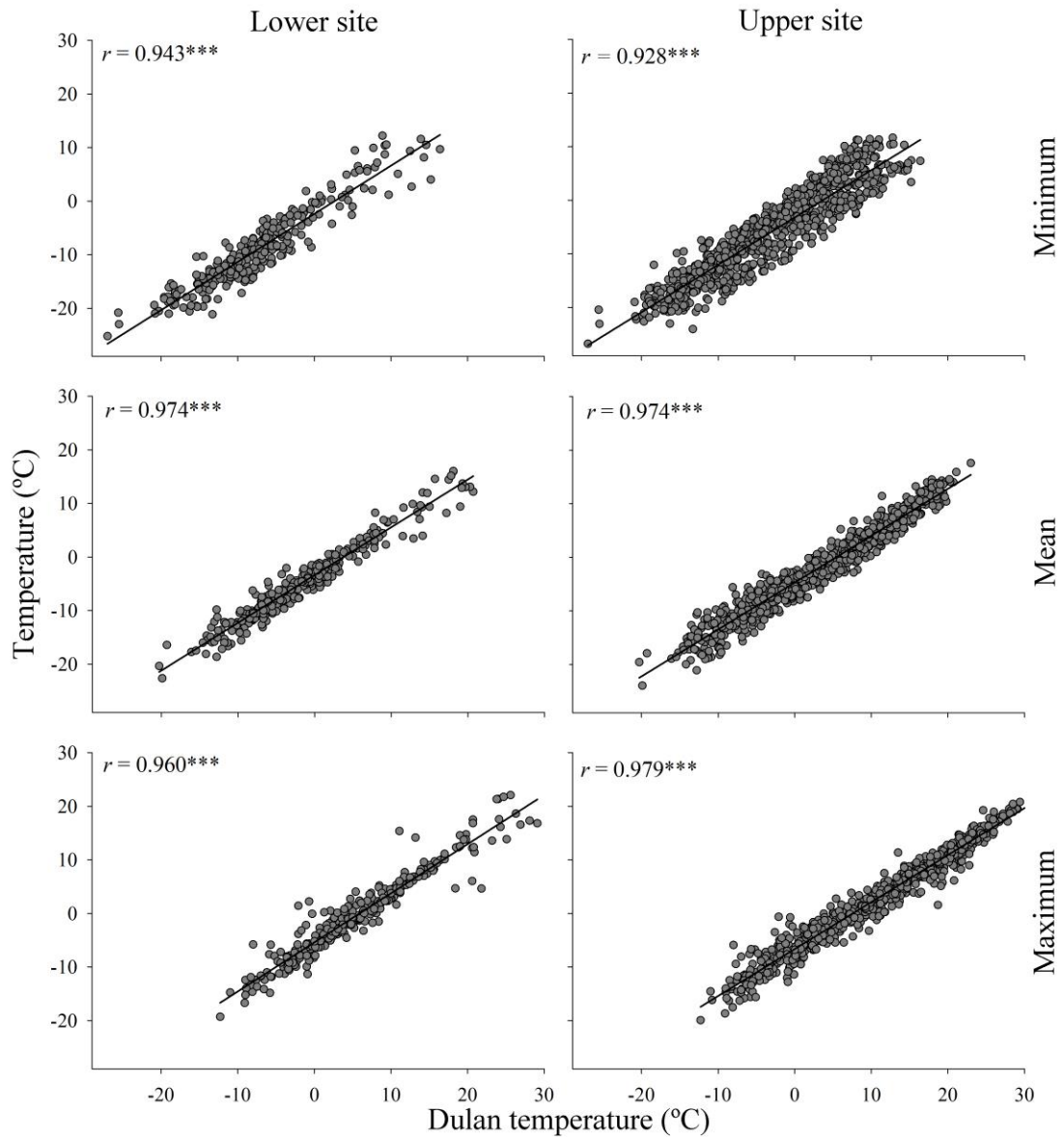
531

532 Fig. S4 The distribution of standardized residuals in the time window of 12 days as a
533 function of minimum, mean and maximum temperatures.

534

535

536

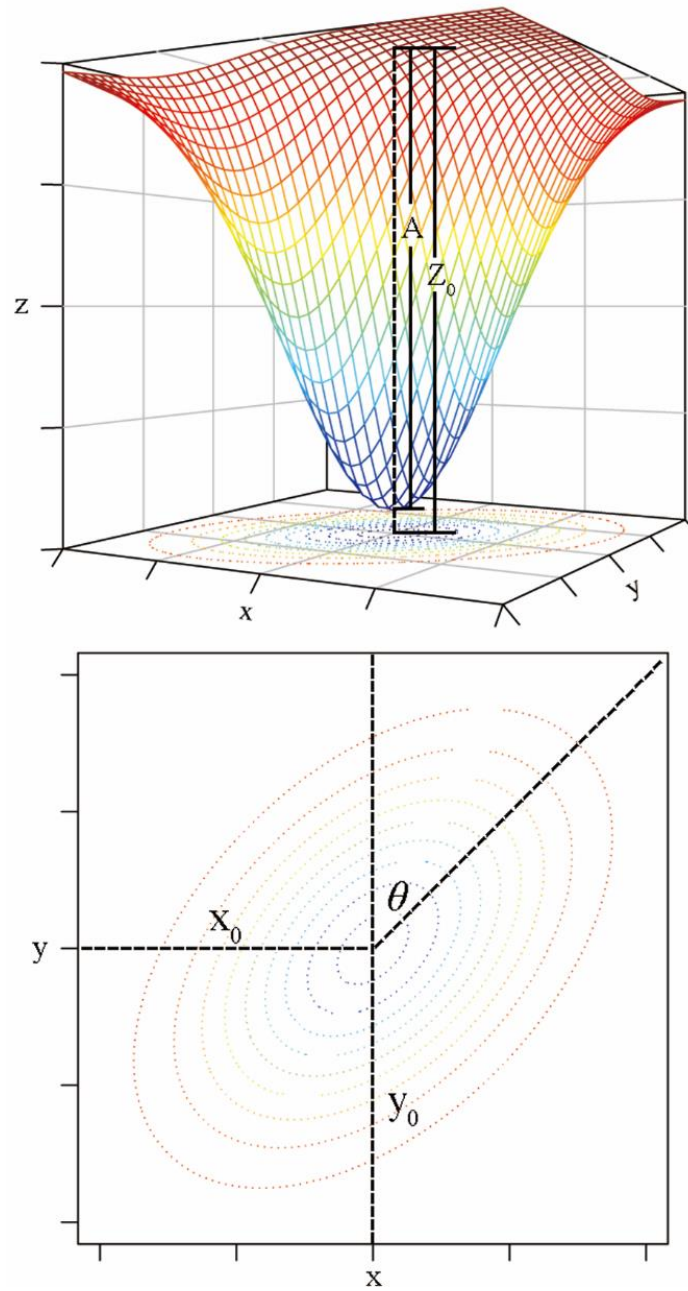


541 Fig. S1 Correlations between the daily minimum, mean and maximum temperatures

542 recorded at the Dulan meteorological station and the corresponding temperatures

543 recorded during 2012-2014 at the lower and upper study sites. ***, correlation

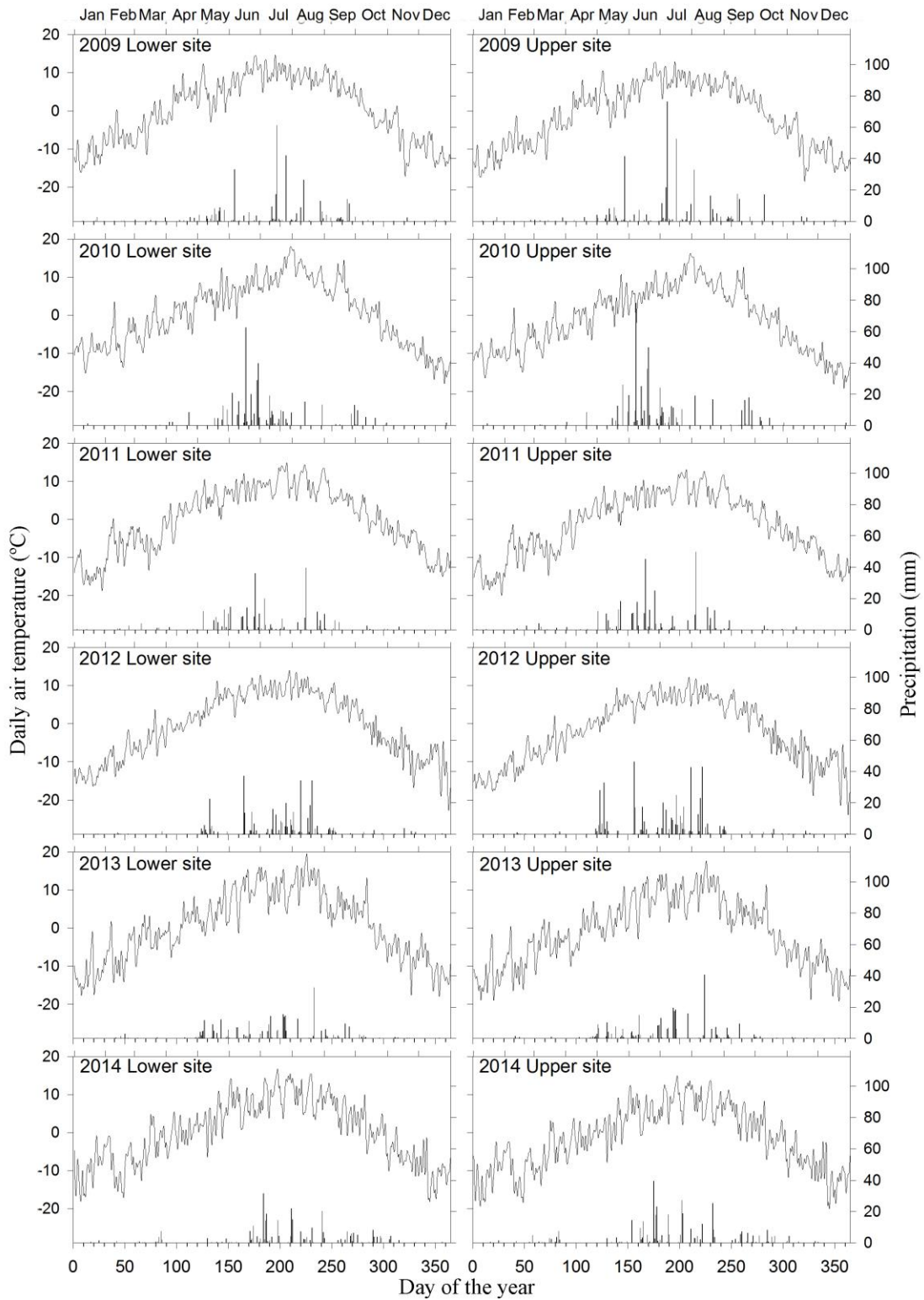
544 coefficients (r) at $P < 0.001$.



546

547 Fig. S2 Sample surface plot and the corresponding level sets of a two-dimensional
 548 Gaussian model. In the upper plot, Z_0 is the distance from the edge of the surface to
 549 the plane ($z = 0$), and A is the height of the trough. In the lower plot, x_0 and y_0 are the
 550 coordinates defining the position of the center of the surface, and θ is the clockwise
 551 rotation angle of the surface.

552

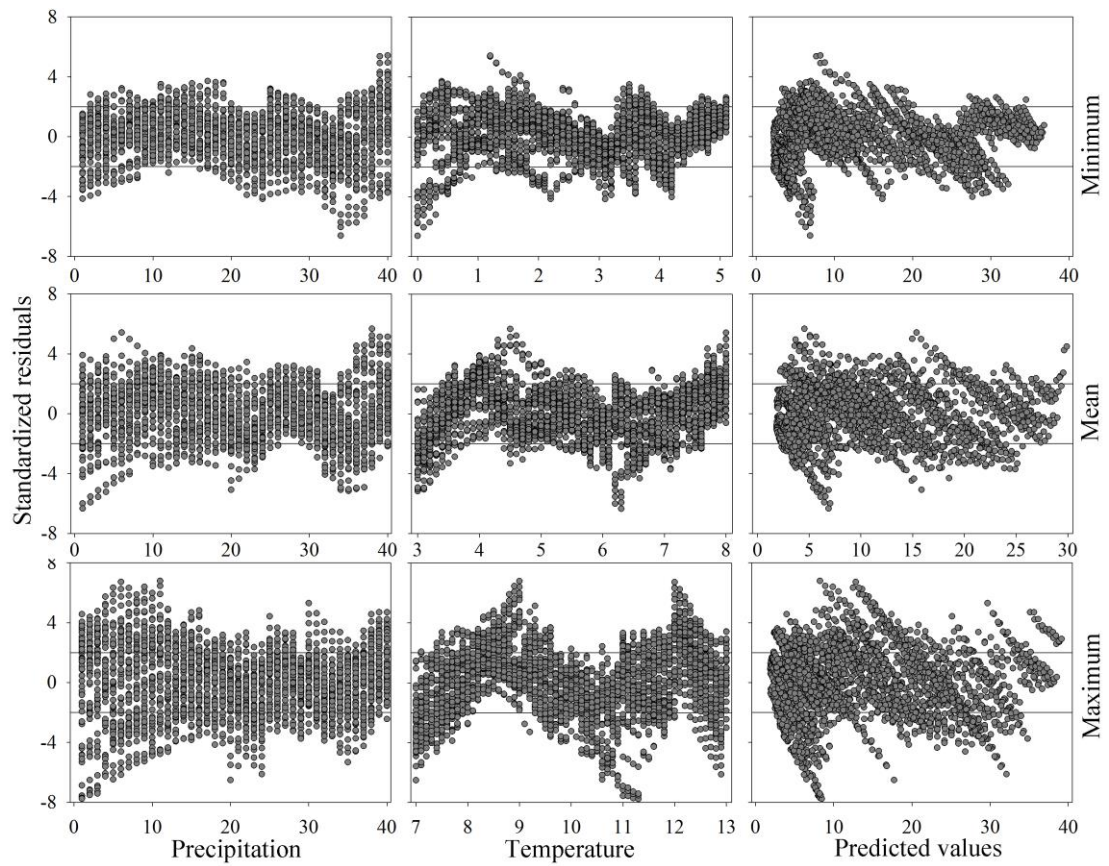


553

554 Fig. S3 Daily air temperature (lines) and precipitation (bars) during 2009-2014 at the
 555 lower and upper study sites.

556

557



558

559

560 Fig. S4 The distribution of standardized residuals in the time window of 12 days as a

561 function of minimum, mean and maximum temperatures.

562